Cell

Genome-wide Mapping and Characterization of Notch-Regulated Long Noncoding RNAs in Acute Leukemia

Thomas Trimarchi,[1,2] Erhan Bilal,[3] Panagiotis Ntziachristos,[1,2] Giulia Fabbri,[4] Riccardo Dalla-Favera,[4] Aristotelis Tsirigos,[2,5,*] and Iannis Aifantis[1,2,*]
[1]Howard Hughes Medical Institute, Laura and Isaac Perlmutter Cancer Center, and Helen L. and Martin S. Kimmel Center for Stem Cell Biology
[2]Department of Pathology
NYU School of Medicine, 550 First Avenue, New York, NY 10016, USA
[3]Computational Biology Center, IBM Thomas J. Watson Research Center, 1101 Kitchawan Road, Yorktown Heights, NY 10598, USA
[4]Institute for Cancer Genetics and the Herbert Irving Comprehensive Cancer Center, Columbia University, 1130 St. Nicholas Avenue, New York, NY 10032, USA
[5]Center for Health Informatics and Bioinformatics, NYU School of Medicine, 227 East 30th Street, New York, NY 10016, USA
*Correspondence: aristotelis.tsirigos@nyumc.org (A.T.), iannis.aifantis@nyumc.org (I.A.)
http://dx.doi.org/10.1016/j.cell.2014.05.049

SUMMARY

Notch signaling is a key developmental pathway that is subject to frequent genetic and epigenetic perturbations in many different human tumors. Here we investigate whether long noncoding RNA (lncRNA) genes, in addition to mRNAs, are key downstream targets of oncogenic Notch1 in human T cell acute lymphoblastic leukemia (T-ALL). By integrating transcriptome profiles with chromatin state maps, we have uncovered many previously unreported T-ALL-specific lncRNA genes, a fraction of which are directly controlled by the Notch1/Rpbjκ activator complex. Finally we have shown that one specific Notch-regulated lncRNA, *LUNAR1*, is required for efficient T-ALL growth in vitro and in vivo due to its ability to enhance *IGF1R* mRNA expression and sustain IGF1 signaling. These results confirm that lncRNAs are important downstream targets of the Notch signaling pathway, and additionally they are key regulators of the oncogenic state in T-ALL.

INTRODUCTION

T cell acute lymphoblastic leukemia (T-ALL) is an aggressive hematological neoplasm that results from the malignant transformation of T-lymphocyte progenitors. T-ALL accounts for only 15%–20% of all acute lymphoblastic leukemia (ALL) cases and is associated with a disproportionate amount of treatment failures and increased mortality. Although the genetic events leading to transformation in T-ALL are complex, aberrant NOTCH1 signaling is a unifying feature, with activating mutations found in more than 50% of cases (Ferrando, 2009; Weng et al., 2004). Previous efforts by our group and others have aimed at dissecting additional genetic (De Keersmaecker et al., 2013; Ntziachristos et al., 2012; Zhang et al., 2012) and molecular (Ferrando et al., 2002; Look, 2004) changes that contribute to induction of T-ALL. Such efforts have yielded important prognostic tools and a more complete understanding of the molecular basis of ALL, including the identification of T-ALL oncogenes (*NOTCH1, MYC*) and tumor suppressors (*FBXW7, CYLD, EZH2, SUZ12*) and the identification and characterization of the leukemia-initiating cell (King et al., 2013). To date, most efforts toward understanding T-ALL have focused on genetic and epigenetic alterations, which ultimately impact function of protein-coding genes. Additionally, several groups have investigated the involvement of noncoding microRNAs (miRNAs) in T-ALL (Fragoso et al., 2012; Li et al., 2011; Yu et al., 2011); however, the requirement of other classes of noncoding RNA for T cell transformation and maintenance has not been investigated thus far.

Recent evidence has revealed that a large portion of the human genome is transcriptionally active despite the fact that only a small portion contains protein-coding genes (Carninci et al., 2005; Clark et al., 2011; Djebali et al., 2012; Katayama et al., 2005). This observation has led many to hypothesize that both human and mouse genomes contain thousands of long noncoding RNA (lncRNA) genes (Cabili et al., 2011; Guttman et al., 2009). Although some have suggested that a subset of lncRNAs are the result of divergent transcription at protein-coding gene promoters (Almada et al., 2013; Seila et al., 2008), this does not explain the existence of many intergenic lncRNAs that do not originate from bidirectional promoters (Cabili et al., 2011; Sigova et al., 2013). In general, lncRNAs are a heterogeneous class of transcripts without any single unifying feature except for an arbitrary minimum length of 200 nucleotides and an apparent lack of protein-coding potential (Guttman et al., 2013; Rinn and Chang, 2012; Ulitsky and Bartel, 2013). Despite this, lncRNAs have been shown to be important in development (Boumil and Lee, 2001; Grote et al., 2013; Guttman et al., 2011; Klattenhoff et al., 2013; Kretz et al., 2013; Loewer et al., 2010;

Rinn et al., 2007) and disease (Gomez et al., 2013; Gupta et al., 2010; Huarte et al., 2010; Lee et al., 2012; Yildirim et al., 2013) in many different cell types, suggesting a ubiquitous role in regulation of cellular state. Although the molecular mechanisms by which lncRNAs act are poorly understood, they have been implicated as regulators of diverse cellular processes including regulation of cell cycle (Hung et al., 2011), RNA stability (Kretz et al., 2013), and chromatin structure (Gupta et al., 2010; Lee, 2012; Tsai et al., 2010; Wang et al., 2011b; Yang et al., 2011). Thus, further efforts toward accurate annotation and functional significance of lncRNAs will be critical for our understanding of these processes.

Although several groups have investigated possible roles for lncRNAs as players in the TP53 tumor-suppressor transcriptional program (Huarte et al., 2010; Hung et al., 2011) and solid tumors (Du et al., 2013; Prensner et al., 2011; Prensner et al., 2013; Yang et al., 2013), our overall knowledge of lncRNAs in cancer, including leukemia, remains extremely limited (Garding et al., 2013; Lee et al., 2012). Here we have used multiple genome-wide data sets in order to create the first all-inclusive lncRNA annotation and mapping in human T-ALL. We have used this annotation to examine lncRNA expression profiles in the context of oncogenic NOTCH1 signaling and have identified Notch-dependent lncRNA expression programs that are deregulated in T-ALL. Finally, we used functional studies to identify a T-ALL-specific activator lncRNA that has a key role in promoting tumor maintenance. Altogether these studies provide evidence to support lncRNAs as key regulators of the pathogenic state in acute leukemia and may carry important clinical relevance as biomarkers or future therapeutic targets.

RESULTS

Comprehensive Mapping of lncRNAs in T-ALL

To gain insights into possible functional roles for lncRNAs in T-ALL, we first sought to create a high-quality map of such transcripts for use in subsequent analyses and functional studies. We have achieved this goal by utilizing the workflow outlined in Figure 1A. Briefly, ultra-high-depth RNA-sequencing (RNA-seq) data sets were generated from multiple human T-ALL cell lines and primary leukemia samples. These data were then used to generate the most comprehensive T-ALL transcriptome assembly to date using an "align then assemble" (Trapnell et al., 2010) approach. To isolate only putative lncRNA genes, we removed all known protein-coding genes and retained all transcripts previously reported as lncRNAs or that have not been identified thus far in other annotation efforts. Single-exon transcripts were eliminated to focus on products of splicing events. Finally, because lncRNA transcription has been suggested to occur by a mechanism very similar to that of coding genes (Guttman et al., 2009), we removed any transcript that did not display enrichment of promoter-associated histone modifications (H3K4me3, H3K4me1, H3K27ac). These efforts have yielded a high confidence T-ALL lncRNA annotation comprised of 6,023 isoforms derived from 1,984 unique gene loci. Out of all of these loci, 46% were identified in the GENCODE v18 lncRNA annotation (Harrow et al., 2012) (Figure 1B), suggesting the presence of many novel lncRNAs in T-ALL. Additionally, we have observed that approximately 26% of lncRNAs detected here were expressed in a divergent orientation with respect to protein-coding genes, whereas the remaining 74% were true intergenic gene loci with their own regulatory elements (Figure 1C), and this ratio of divergent to intergenic lncRNAs is approximately the same in T-ALL and normal T cell progenitors (Figure S1D). Additionally, 40% of intergenic lncRNAs were identified by GENCODE, whereas the remaining 60% represent novel lncRNA loci (Figure S1C available online).

We next examined the expression patterns of our T-ALL lncRNA catalog over a diverse panel of cell types including T-ALL, primary T cells, and many other somatic tissues (Human Body Map data). In agreement with previous reports (Cabili et al., 2011), we have observed that average lncRNA expression was lower than protein-coding gene expression (Figure 1D). Additionally, putative lncRNAs showed very little protein-coding potential as measured by the PhyloCSF algorithm (Lin et al., 2011) (Figure S1A). In agreement with possible roles in regulating gene expression, many lncRNAs were enriched in RNA from nuclear extracts compared to total RNA (Figure S1B). Finally, upon examination of the 250 most variable lncRNAs, as measured by quartile coefficient of dispersion, we observed striking specificity for T-ALL and normal T cells (Figure 1E), which is consistent with the notion (Guttman et al., 2009) that lncRNA expression is highly tissue specific. However, many lncRNAs were specifically expressed in human T-ALL when compared to untransformed peripheral T cells (Figure 1E), suggesting that T cell transformation is dynamically changing the lncRNA landscape in this cell type. Overall, this effort cataloged T-ALL-specific noncoding RNAs and represents a comprehensive mapping of lncRNA expression in this aggressive subtype of ALL.

T-ALL-Specific lncRNAs Are Part of the NOTCH1 Oncogenic Network

Given that oncogenic NOTCH1 activity is one of the key features in T-ALL and NOTCH pathway activity characterizes the vast majority (>90%) of human T-ALL cases, we reasoned that the lncRNA expression program in this disease may be influenced by the NOTCH1/RBPJκ transcriptional activator complex. Upon examination of lncRNA promoters, we noticed a high density of NOTCH1/RBPJκ chromatin immunoprecipitation sequencing (ChIP-seq) signal at many of these regions (Figures 2A and 2B). Additionally, most lncRNA promoters displayed high enrichment of H3K4me3, H3K27ac, and RNA polymerase II (RNA PolII) signal proximal to their TSSs. We also observed a subset of lncRNAs, which showed co-occupancy of NOTCH1 and ZNF143 (Figures 2A and S2C), a protein that has been previously reported to co-occupy the genome with Notch, although its role in gene regulation is unclear (Wang et al., 2011a). We therefore hypothesized that expression of a subset of lncRNA genes may be dependent on NOTCH1-mediated signaling. To test this hypothesis, we used chemical inhibition of the γ-secretase complex (Kopan and Ilagan, 2009) to perturb NOTCH1 cleavage and nuclear translocation in two prototypical human T-ALL cell lines (CUTLL1 and HPB-ALL) and carried out RNA-seq to measure lncRNA expression following treatment and NOTCH inhibition. Such approaches have been extensively used in T-ALL and are proven to specifically target NOTCH1

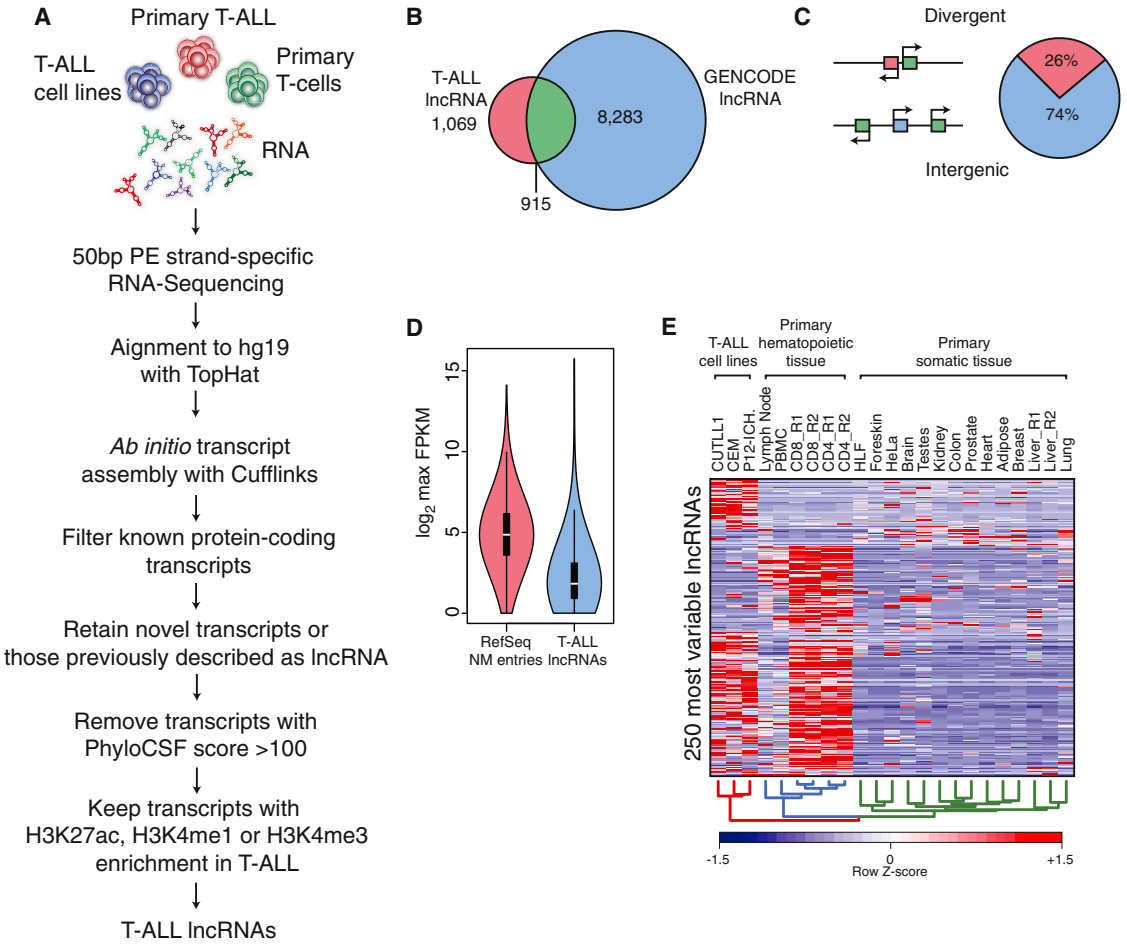

Figure 1. The Long Noncoding Transcriptome in T-ALL

(A) A schematic illustration of the procedure used to discover and define lncRNAs in T-ALL.

(B) Venn diagram depicting the overlap between our catalog of T-ALL-associated lncRNAs and those in the Gencode v18 lncRNA collection.

(C) Pie chart representation showing the proportion of T-ALL-associated lncRNAs that are transcribed in a divergent orientation (red) or intergenic (blue) with respect to protein-coding genes (green, diagram left).

(D) Violin plot of $\log_2$ maximum expression values (FPKM) for protein-coding (red) and T-ALL lncRNA (blue) genes. Boxes represent first and third quartiles. Whiskers are 1.5 times the interquartile range (IQR).

(E) A heatmap representation of the 250 lncRNAs with the most variable (IQR/median) expression across T-ALL, normal T cells, and various other somatic tissues.

signaling (Palomero et al., 2006; Weng et al., 2004). Indeed, we observed that in addition to protein-coding genes, many lncRNA genes were differentially expressed upon γ-secretase inhibitor (γ-SI) treatment compared to vehicle controls (Figures 2C and S2A), suggesting direct regulation and possible roles downstream of NOTCH1 activation in this disease. In agreement with this notion, we observed that approximately 55% of lncRNAs whose expression was Notch dependent were also directly occupied by NOTCH1 (Figure 2D). In support of our hypothesis that NOTCH1 controls the lncRNA transcriptional program in T-ALL, we observed that lncRNAs associated with the top 1,000 most enriched NOTCH1-binding sites were significantly downregulated upon administration of γ-SI according to gene set enrichment analysis (GSEA) (Figure 2E). Upon closer examination of many of these lncRNA loci, we observed strong NOTCH1/RBPJκ-binding sites (Wang et al., 2011a) at both promoters and intragenic enhancer elements (Figure S2B, highlighted yellow), suggesting direct transcriptional control by Notch signaling. Together these data suggest the presence of a Notch-dependent T-ALL lncRNA expression program, members of which, we believe, may carry important biological functions.

To address whether these Notch-regulated lncRNA genes might be expressed in primary NOTCH1-induced T-ALL, we measured their expression across ten patient samples that harbored activating *NOTCH1* mutations as well as two primary human thymus samples, as a matched physiological tissue with low Notch activation (Ntziachristos et al., 2012). These analyses yielded a subset of lncRNAs that displayed differential expression in primary T-ALL compared to normal thymic T cells (Figure 2F). We also observed that a subset of lncRNAs are differentially expressed among distinct subtypes of T-ALL

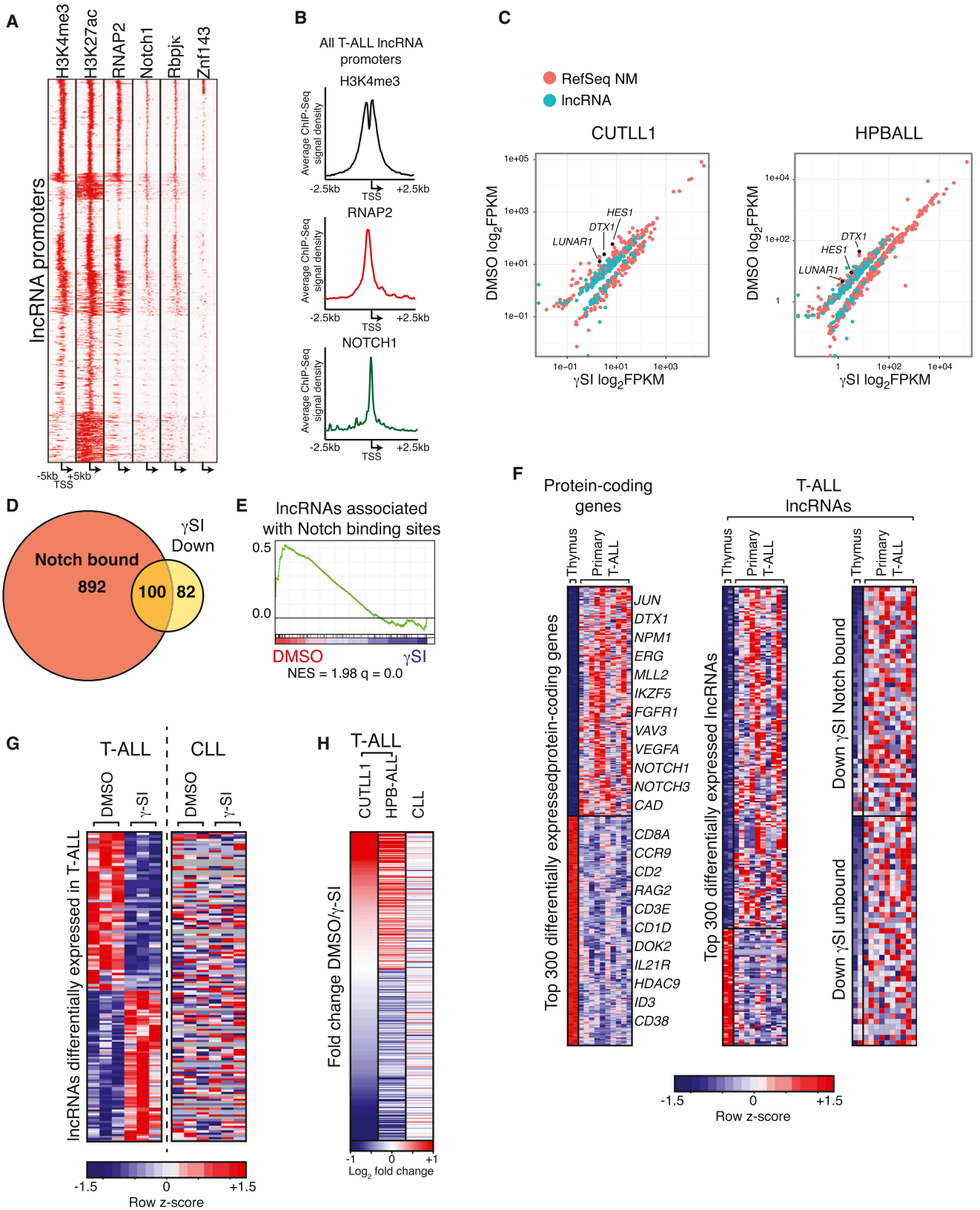

(legend on next page)

as defined by aberrant expression of *TLX1* or *TLX3* (Figure S2D), suggesting a possible role in specifying discreet subclasses within this disease.

Given that activating mutations on NOTCH1 have been recently discovered in chronic lymphocytic leukemia (CLL) (Fabbri et al., 2011), a tumor of the B-lymphocyte compartment, we hypothesized that Notch-dependent lncRNAs that we have described in T-ALL might also show similar expression patterns in CLL. To test this hypothesis, we cultured Notch mutant CLL cells on OP9-DL1 stromal cells, which express the Notch ligand delta-like 1 (DL1), and added vehicle control (DMSO) or γ-SI followed by RNA-seq (Figure 2G). By comparing our T-ALL and CLL γ-SI treatment experiments, we observed that Notch-dependent changes in lncRNA expression in T-ALL are different from those in CLL (Figures 2G and 2H). To our surprise, we observed very little conservation of the Notch-dependent T-ALL lncRNA expression program in Notch mutant CLL cells, suggesting that although these two tumors harbor similar oncogenic lesions, the downstream consequences of Notch activation are distinct.

LUNAR1 Is a NOTCH-Regulated lncRNA Transcript in Human T-ALL

Because lncRNAs have been previously shown to enhance expression of nearby genes through *cis*-regulation (Gomez et al., 2013; Lai et al., 2013; Ørom et al., 2010), we next asked whether any of the lncRNAs identified here display a high Pearson correlation with neighboring protein-coding genes. By comparing correlation density plots for all coding/lncRNA and coding/coding gene pairs, we found that in general, lncRNAs are no more correlated with neighboring genes than their coding counterparts (Figure 3A). However, because enhancer-like activity for lncRNAs has been proposed before, we considered all lncRNAs with at least 0.75 correlation (Figure 3A, shaded area) with a coding neighbor as candidates for further study as *cis*-regulators. From these candidates, we noticed one lncRNA gene, which we have termed *LUNAR1* (*leu*kemia-induced *n*oncoding *a*ctivator *R*NA), that showed high correlation with its coding neighbor gene the insulin-like growth factor receptor 1 (*IGF1R*) (r = 0.77), a gene which has been previously suggested to play a role in T-ALL (Medyouf et al., 2011). We noted several other features that made *LUNAR1* appear attractive as a candidate. It was downregulated upon Notch inhibition (Figure 3C), overexpressed in primary T-ALL (Figure 3B), and expressed significantly higher in T-ALL samples that harbored a Notch mutation compared to those without mutations (Figure 3D). Additionally, we also found an enrichment of *LUNAR1* in the nucleus (Figure 3E), to a degree similar to that of *U1*, a component of a small nuclear ribonucleoprotein (snRNP) splicing complex, which supported our hypothesis that this transcript may be involved in gene regulation. By examining the chromatin state at the *LUNAR1* locus, we observed typical features of RNAP2-dependent genes in T-ALL (Figure S3A), as well as a transcriptionally active state in several related hematopoietic cell types, according to the chromHMM algorithm (Figure S3B). Although a transcriptionally active chromatin state was restricted to very few samples, nearly all of the cell types for which chromHMM data were available showed signs of active promoter-associated chromatin structure proximal to the *LUNAR1* TSS, indicating a true transcriptional unit (Figure S3B). Although the *LUNAR1* locus shows signs of promoter activity in diverse tissues, its expression is highly restricted, suggesting that specific factors are required for its activation. Using standard 5′ and 3′ rapid amplification of cDNA ends (RACE) approaches, we were able to clone a 491-nucleotide transcript containing 4 exons and a poly(A) tail (FASTA sequence in supplement). In order to address whether *LUNAR1* is indeed noncoding, we utilized the PhyloCSF algorithm (Lin et al., 2011), which yielded a score of −48.12, indicating lack of an open reading frame (ORF) with selective pressure for codon preservation. Additionally, we used PFAM to translate the RNA sequence in three frames and searched for known protein domains, of which we found none (not shown). These data strongly suggest that the *LUNAR1* transcript is unlikely to encode any protein product.

LUNAR1 Expression Is Controlled by an Intronic Enhancer in the *IGF1R* Locus

To further study possible functional significance of *LUNAR1*, we utilized genome-wide chromosome conformation capture (Hi-C) in T-ALL cells (CUTLL1) to examine the higher-order chromatin context in T-ALL (I.A., P.N., and A.T., unpublished data). Similar to other chromosome capture methods, Hi-C utilizes restriction enzyme digestion of crosslinked chromatin followed by intramolecular ligation to physically link genomic regions that were in close spatial proximity to one another (Lieberman-Aiden et al., 2009). By coupling this method to high-throughput sequencing, we created a map of 3D chromatin structure in human T-ALL cells. In doing so, we discovered that *LUNAR1* resides in a 500 kb topologically associating domain (Dixon et al., 2012) on chromosome 15, which also includes neighboring genes *IGF1R* and *PGPEP1L* (Figure 4A). Of these two neighboring genes, only *IGF1R* is transcriptionally active; therefore we reasoned that *LUNAR1* might play a role in enhancing

Figure 2. lncRNAs Are a Component of the Notch1 Transcriptional Network

(A) Heatmap representation of ChIP-seq signal density for H3K27ac, H3K4me3, RNAP2, NOTCH1, RBPJκ, and ZNF143 centered on lncRNA TSSs ± 5 kb. All ChIP experiments are from CUTLL1 cells.

(B) Histogram depicting ChIP-seq signal density on all T-ALL lncRNA promoters for H3K4me3, RNAP2, and NOTCH1.

(C) Scatterplots showing both lncRNA (green) and protein-coding (orange) genes whose expression is significantly altered following addition of γ-SI in CUTLL1 (left) and HPBALL (right) cells.

(D) Venn diagram showing the proportion of Notch-occupied lncRNAs whose expression is significantly downregulated in response to γ-SI treatment.

(E) GSEA enrichment plot showing significant downregulation of lncRNAs associated with the top 1,000 NOTCH1 peaks upon γ-SI treatment.

(F) Heatmaps showing top differentially expressed protein-coding (left) and lncRNA (right) genes in primary T-ALL compared to thymic progenitors.

(G) Expression profiles of lncRNAs that are differentially expressed in response to γ-SI treatment in T-ALL are shown in heatmap either in T-ALL (left) or CLL (right). Gray indicates no detectable expression.

(H) Expression fold-change (DMSO/γ-SI) in T-ALL (CUTLL1 And HPBALL) and CLL of all lncRNAs consistently regulated upon Notch inhibition in T-ALL.

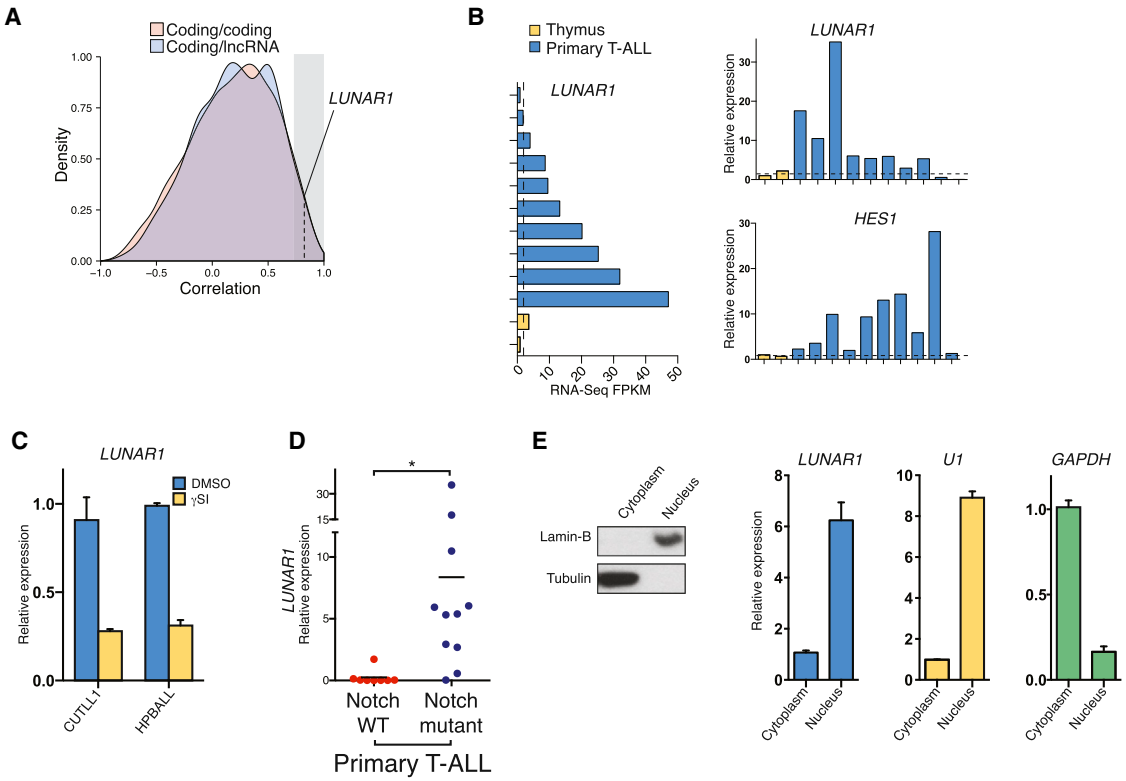

Figure 3. *LUNAR1* Is a lncRNA Gene Controlled by NOTCH1 in T-ALL

(A) Correlation density plot showing expression correlation of protein-coding (red) or lncRNA (blue) genes with the nearest coding neighbor.

(B) RNA-seq expression values for *LUNAR1* in primary T-ALL and thymic progenitors (left). Overexpression was validated by qPCR (right, top), and overactivation of Notch signaling was verified by measuring *HES1* expression (bottom, right).

(C) qPCR for *LUNAR1* following treatment with vehicle (blue) or γ-SI (red) in CUTLL1 (left) and HPBALL (right) cells.

(D) qPCR for *LUNAR1* in Notch wild-type (WT) versus Notch mutant tumors.

(E) Immunoblot (left) for lamin B and tubulin on cytoplasmic and nuclear fractions from CUTLL1 cells. qPCR (right) for *LUNAR1, U1*, and *GAPDH* from RNA extracted from cytoplasmic and nuclear fractions. * indicates p value < 0.05.

Error bars represent SEM of three experiments.

expression of this gene. Closer examination of the *LUNAR1/IGF1R* locus revealed the presence of a highly active enhancer in the last intron of *IGF1R,* which showed a high degree of occupancy by NOTCH1 (previously reported; Medyouf et al., 2011), Mediator subunit MED1, histone acetyltransferase P300, RNA PolII, and the histone reader BRD4 (Figures 4B and S4A), all of which have been suggested to be hallmarks of active enhancer elements when located outside of promoter regions (Heintzman et al., 2009; Rada-Iglesias et al., 2011; Whyte et al., 2013). In addition to showing enrichment for enhancer-associated chromatin factors and a chromatin signature characteristic of active enhancer elements (high H3K4me1, low H3K4me3, high H3K27ac), we showed that this element is able to drive expression in a reporter assay in a Notch-dependent manner (Figures S4B and S4C).

We used chromosome conformation capture (3C) followed by quantitative PCR (qPCR) to validate our Hi-C findings and identified a peak of high crosslinking frequency at the *IGF1R* enhancer when using a constant HindIII fragment located close to the *LUNAR1* promoter, indicating the presence of a chromatin loop that places these regions in close physical proximity within the 3D organization of the nucleus (Figure 4C). This finding was verified using a constant HindIII fragment in the *IGF1R* enhancer, suggesting a specific interaction (Figure 4C, lower panel). These results suggest that this Notch-occupied enhancer element in the *IGF1R* locus is able to control *LUNAR1* expression through promoter/enhancer contacts.

LUNAR1 Controls *IGF1R* Expression and Is Essential for T-ALL Maintenance

To provide evidence further supporting a more causal relationship between *LUNAR1* and *IGF1R*, we used RNAi to attenuate *LUNAR1* expression. In doing so, we noticed that abrogation of *LUNAR1* led to repression of *IGF1R*, an effect that was observed using two independent small hairpin RNAs (shRNAs) targeting distinct regions of the transcript (Figure 5A). Ectopic expression of *LUNAR1* using retroviral vectors, which integrate randomly into the genome, did not yield significantly different expression of *IGF1R* mRNA (Figure S5A), supporting our hypothesis of a *cis*-activation mechanism. Additionally, *LUNAR1* depletion resulted in a competitive growth disadvantage phenotype in T-ALL cells (CUTLL1, HPB-ALL) in which the transcript is highly

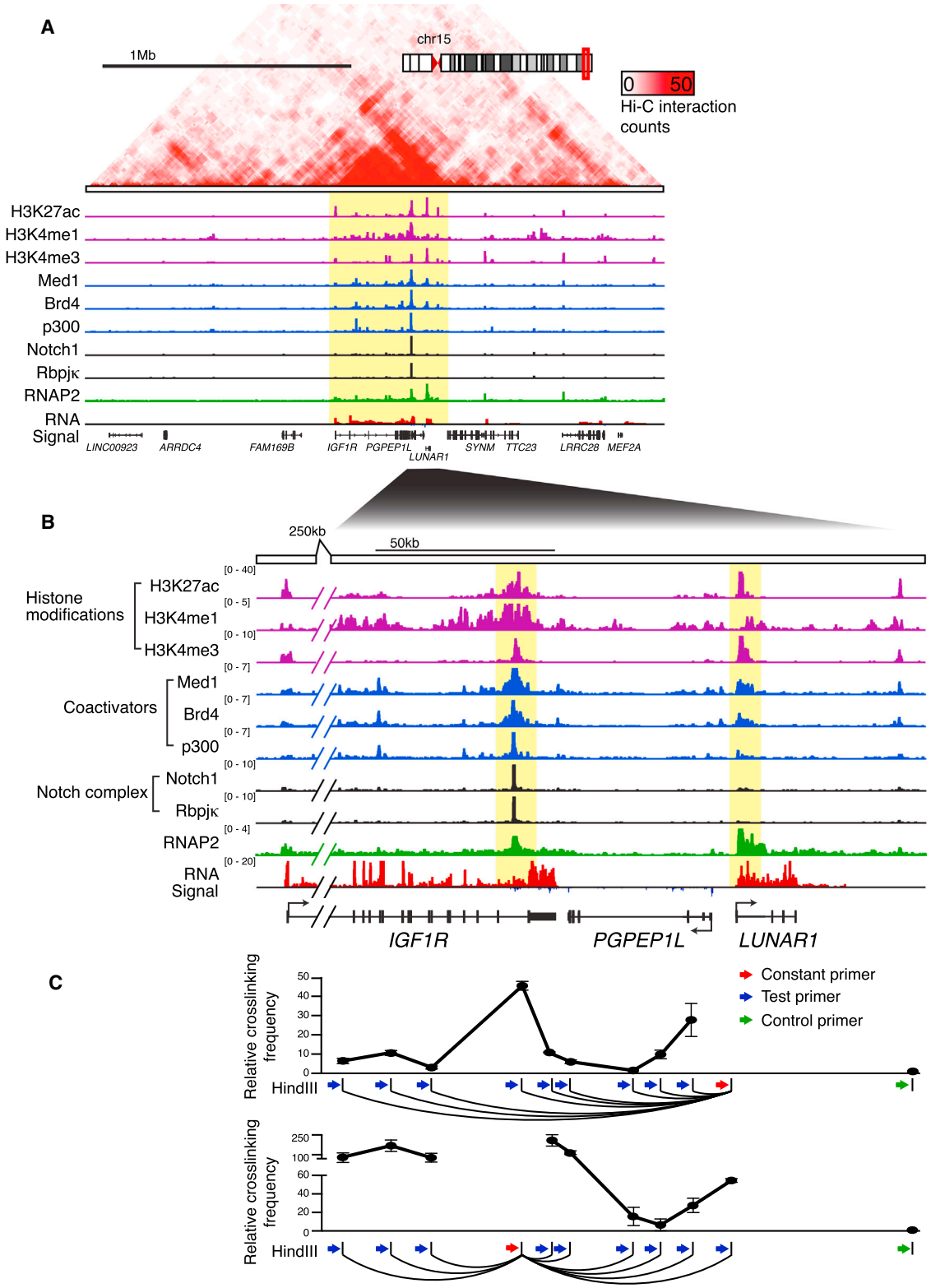

Figure 4. *LUNAR1* Is Physically Associated with a Nearby Notch-Occupied Enhancer

(A) Gene track of a 2 Mb region surrounding the *LUNAR1* locus including Hi-C interaction density heatmap (red upper panel), ChIP-seq tracks for H3K27ac, H3K4me1, H3K4me3, MED1, BRD4, P300, NOTCH1, RBPJκ, and RNAP2, and RNA-seq track.

(legend continued on next page)

expressed (Figure 5B) but did not lead to a similar phenotype in myeloid leukemia cells (HL-60) (Figure S5B), in which *LUNAR1* expression is limited, suggesting on-target and T-ALL-specific effects (Figure 5B). Depletion of *LUNAR1* caused a significant decrease in the number of actively cycling cells as shown by 7AAD staining (Figure S5E). These T-ALL growth effects were similar to the ones noted when the *IGF1R* gene was silenced ((Medyouf et al., 2011 and data not shown). In order to further rule out off-target effects of RNAi, we utilized antisense DNA/RNA hybrid oligonucleotide (ASO) gene-silencing technology, which triggers RNase-H-mediated degradation of the target transcript upon ASO binding. ASO-mediated depletion of *LUNAR1* led to both repression of *IGF1R* mRNA (Figure S5C) and a growth retardation phenotype similar to what we observed with RNAi (Figure S5D).

In order to test the effects of *LUNAR1* depletion on tumor growth in vivo, we performed xenograft assays in which human T-ALL cells expressing an shRNA targeting *LUNAR1* (GFP) or Renilla (mCherry) control were mixed at a 1:1 ratio and transferred intravenously into sublethally irradiated immunodeficient hosts (Figure 5C). Four weeks after the transplantation, we harvested peripheral tumors and measured by fluorescence-activated cell sorting (FACS) analysis the relative contribution of cells harboring each shRNA. Using this assay, we observed a significant loss of representation of cells in which *LUNAR1* was depleted (Figure 5D), which suggested that this lncRNA is required for efficient tumor growth both in vitro and in vivo.

To test whether *IGF1R* is the relevant target of *LUNAR1* as we have hypothesized, we performed ASO-mediated lncRNA depletion in T-ALL cells ectopically expressing *IGF1R* using retroviral constructs or empty vector control. Following ASO delivery, we observed that ectopic expression of *IGF1R* efficiently rescued the growth defects observed following *LUNAR1* depletion (Figure 5E), suggesting that *IGF1R* is indeed a key target of this lncRNA.

To characterize the overall cellular response to *LUNAR1* silencing, we performed global gene-expression analysis (RNA-seq) in T-ALL cells following *LUNAR1* depletion with two independent shRNAs. For comparison, we also performed experiments in which we blocked IGF1 signaling using pharmacological inhibition (BMS-536924) followed by RNA-seq. The outcome of these studies was striking as we noted significant repression of *IGF1R* mRNA, in agreement with our qPCR studies (Figure 5A). We also identified a subset of genes, which were similarly regulated following either *IGF1R* inhibition or *LUNAR1* depletion (Figure 5F), suggesting that this lncRNA promotes IGF1 signaling by transcriptional regulation of *IGF1R*. Finally, using GSEA, we found significant enrichment for gene sets containing genes significantly downregulated upon IGF1 inhibition in T-ALL (Figure S5F) and other publicly available gene sets containing targets of IGF1/2 (Figure S5F).

LUNAR1 Is an Activator RNA Capable of Stimulating Gene Activity

In order to test whether *LUNAR1* displayed intrinsic ability to promote gene activity, we used the Gal4-λN/BoxB system to tether this lncRNA to a heterologous reporter promoter (Li et al., 2013; Wang et al., 2011b). In this system, the BoxB RNA stem loop is fused to a lncRNA, which allows it to bind specifically and with high affinity to the phage λ N-peptide (λN). By fusing λN to the DNA-binding domain of the yeast Gal4 protein, a BoxB-tagged lncRNA can be tethered to UAS DNA sequences (Figure 6A). We cotransfected vector containing the Gal4-λN fusion with either BoxB-tagged *LUNAR1* or known activator lncRNA *HOTTIP* into HEK293 cells stably expressing five UAS sites upstream of a TK-luciferase reporter gene (Vaquero et al., 2004). Upon transfection, we could detect binding of the Gal4-λN fusion at the reporter promoter as expected (Figure 6B). Tethering *LUNAR1* to this reporter gene stimulated transcription of the reporter to a similar degree as *HOTTIP* (Figure 6C). Additionally, ASO-mediated depletion of *LUNAR1* (Figure 6D) significantly reduced this stimulatory effect compared to a nontargeting ASO (Figure 6E), suggesting that molecules of *LUNAR1* are functionally important for the stimulation of transcription seen here.

In order to investigate the mechanism by which endogenous *LUNAR1* promotes transcriptional activity of the *IGF1R* gene, we performed chromatin studies following depletion of the lncRNA in T-ALL cells. Because we hypothesized that *LUNAR1* might be an important component of the intronic *IGF1R* enhancer, we reasoned that depletion of this transcript might influence chromatin state or occupancy of one of the activators at that locus. Following depletion of *LUNAR1*, we observed a significant reduction in Mediator complex (MED1 and MED12) and RNA PolII occupancy at both the *IGF1R* enhancer and the *LUNAR1* promoter (Figures 7A and 7B). Additionally, we observed significant loss of RNA PolII binding at the *IGF1R* promoter (not shown). We did not observe any changes in NOTCH1 binding or levels of histone modifications H3K27ac, H3K4me1, or H3K4me3 at these loci (Figures 7A and 7B), suggesting specific destabilization of Mediator and RNAP2 following *LUNAR1* depletion. We observed no changes in the status of any of these factors at the *ACTB* promoter, again suggesting a locus-specific effect. Because depletion of *LUNAR1* led to locus-specific loss of Mediator and RNA PolII binding, we hypothesized that *LUNAR1* RNA might co-occupy the chromatin in those loci. Using chromatin isolation by RNA purification (ChIRP), we were able to efficiently retrieve *LUNAR1* RNA (Figure 7D) and observed specific enrichment of *LUNAR1* at the *IGF1R* enhancer and *LUNAR1* promoter (Figure 7E), which supports a mechanism by which *LUNAR1* exploits chromatin configuration to reach its targets (Figure 7F) (Engreitz et al., 2013). Together these data suggest that the intronic *IGF1R* enhancer activates *LUNAR1,* which then co-occupies the element and further recruits Mediator in order to sustain full activation of the *IGF1R* promoter.

(B) Gene track view of an approximately 150 kb region that contains *LUNAR1* (highlighted yellow, right) and a Notch-occupied enhancer in the last intron of *IGF1R* (highlighted yellow, left).

(C) Relative crosslinking frequency as measured by 3C-qPCR using a constant primer in a HindIII fragment at the *LUNAR1* TSS (top) or at the Notch-occupied enhancer (bottom). Crosslinking frequency is relative to a negative region (green).

Error bars indicate the ± SEM of three experiments.

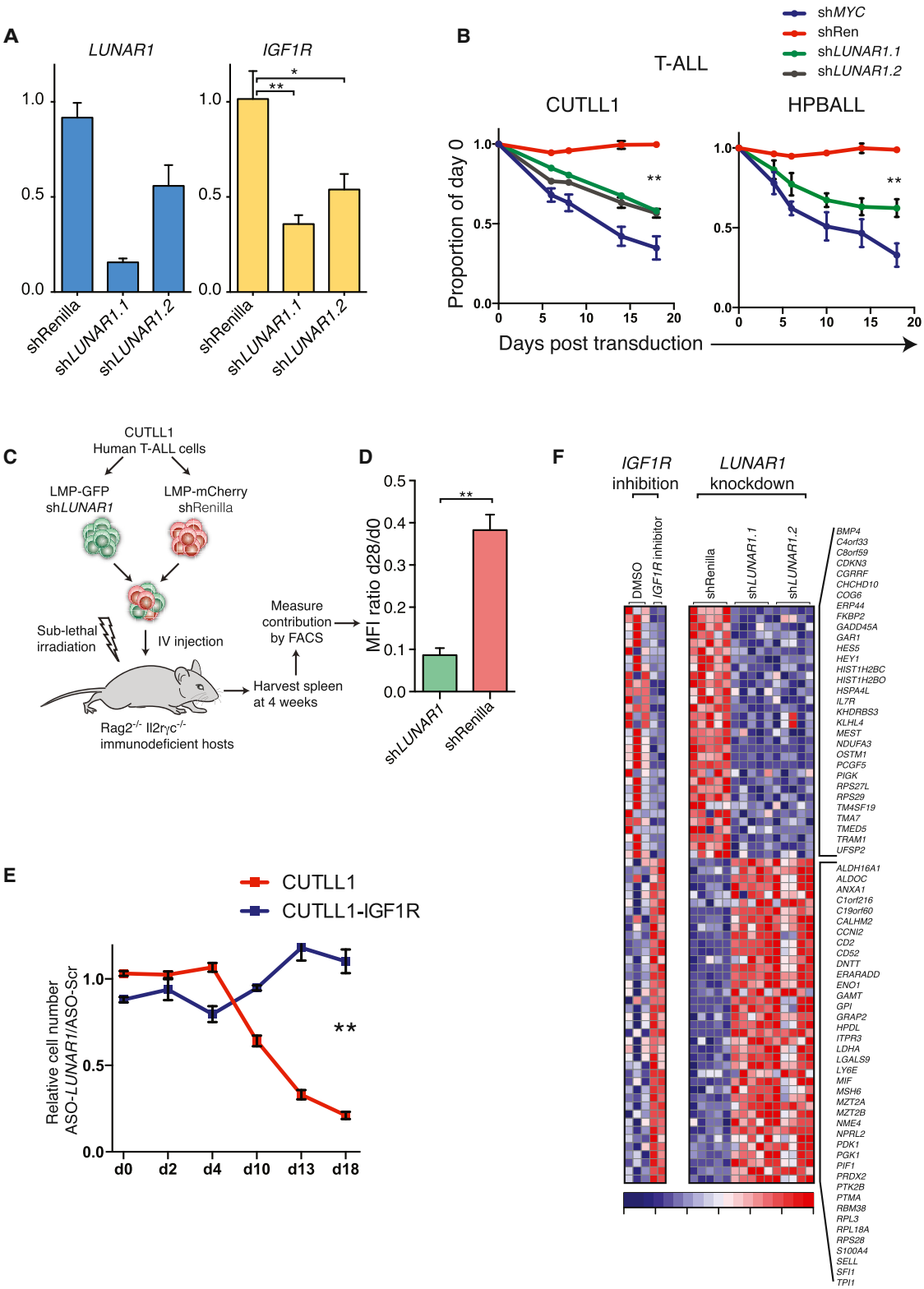

Figure 5. *LUNAR1* Regulates T-ALL Proliferation by Enhancing *IGF1R* Expression

(A) qPCR showing expression of *LUNAR1* (blue) and *IGF1R* (yellow) in the presence of shRNAs targeting Renilla or *LUNAR1*.

(B) Line graphs showing relative contribution from T-ALL cells expressing shRNAs against *LUNAR1* grown in competition with cells expressing a nontargeting shRNA.

(legend continued on next page)

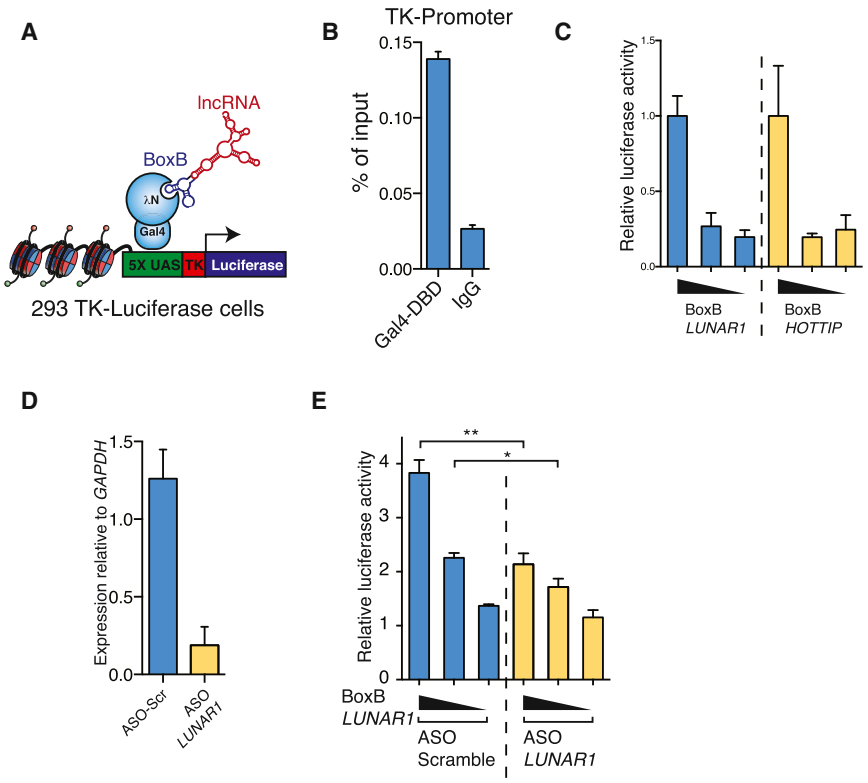

Figure 6. *LUNAR1* Is Able to Stimulate Transcription of a Reporter Gene

(A) Illustration describing the BoxB Gal4-λN RNA tethering system used.

(B) ChIP assay for Gal4-DBD at the reporter gene promoter.

(C) Luciferase reporter activity in experiments where BoxB-tagged *LUNAR1* (blue) or *HOTTIP* (yellow) were cotransfected with Gal4-λN.

(D) qPCR following ASO knockdown of *LUNAR1* in luciferase assay.

(E) Reporter assay showing relative reporter gene activity when BoxB-*LUNAR1* was cotransfected with either nontargeting (blue) or *LUNAR1*-specific (yellow) ASOs.

Error bars represent SEM of at least three experiments. * indicates p value < 0.05. ** indicates p value < 0.01.

These studies revealed *LUNAR1* as a regulator of IGF1 signaling and T-ALL cell growth, identifying a putative lncRNA that could be therapeutically targeted in acute leukemia. Additionally we provide further evidence for the ubiquitous presence and functional importance of lncRNAs in human disease and provide evidence that lncRNAs, in addition to protein-coding genes, are key downstream targets of Notch signaling.

DISCUSSION

The last decades were characterized by an extensive delineation of oncogenic pathways in different cancer types, focusing on protein-coding transcripts and more recently on noncoding miRNA networks. However, very little was known on expression patterns and biological significance of lncRNAs in human tumorigenesis. Also, very little was reported on the regulation of such lncRNAs by well-described oncogenic signaling pathways. Here we map the expression of lncRNAs in acute leukemia, using T-ALL, a disease characterized by activation of the NOTCH pathway. Using integration of whole transcriptome analysis and genome-wide chromatin state maps, we systematically identified T-ALL-specific lncRNA genes and characterized noncoding transcripts regulated directly by the binding and the activation of NOTCH1. To further suggest biological significance, we used RNA-seq of primary human T-ALL, characterized by NOTCH1 and FBXW7 mutations (leading to NOTCH activation), and were able to prove the existence of T-ALL-specific lncRNAs also regulated by NOTCH1 activity, suggesting that NOTCH signaling is able to shape not only the protein-coding but also the lncRNA landscape in this disease. These results suggest that—at least a fraction of—the NOTCH1-triggered oncogenic activity could be due to its ability to regulate such noncoding transcripts.

To test this assumption, we have selected *LUNAR1*, a lncRNA that shows T-ALL-specific Notch-dependent expression patterns, is localized in the nucleus, and displays high correlation with *IGF1R,* a receptor previously suggested to play a role in T-ALL (Medyouf et al., 2011). Using assays that can map chromosome conformation and looping, we were able to show an interaction between the TSS of *LUNAR1* and an enhancer element located within the *IGF1R* locus, characterized by NOTCH1 binding (Figures 4 and S4). To prove the connection between *LUNAR1* expression and *IGF1R*, we were able to demonstrate that the silencing of this lncRNA led to a significant downregulation of *IGF1R* expression in T-ALL cells and diminished IGF1 pathway activity. Although it is possible that *IGF1R* is not the sole target of *LUNAR1*, we propose that one of its key functions is to modulate IGF1 signaling in T-ALL by regulation transcription of the receptor gene (Figure 5).

Using various assays (Figures 6 and 7), we have provided evidence that *LUNAR1* belongs to a subclass of enhancer-like lncRNAs, which have been reported previously (Lai et al., 2013; Ørom et al., 2010; Wang et al., 2011b; Yang et al., 2014).

(C) Illustration describing in vivo xenograft competition assay.

(D) Ratio of mean fluorescence intensity (MFI) on day 28:day 0.

(E) Line graphs showing relative cell number (targeting/Scr) for cells expressing exogenous *IGF1R* (blue) or empty vector (red) treated with ASO.

(F) Genome-wide measurement of differentially expressed genes following pharmacological inhibition of *IGF1R* or *LUNAR1* knockdown.

Error bars represent ± SEM of at least three experiments. * indicates p value < 0.05. ** indicates p value < 0.01.

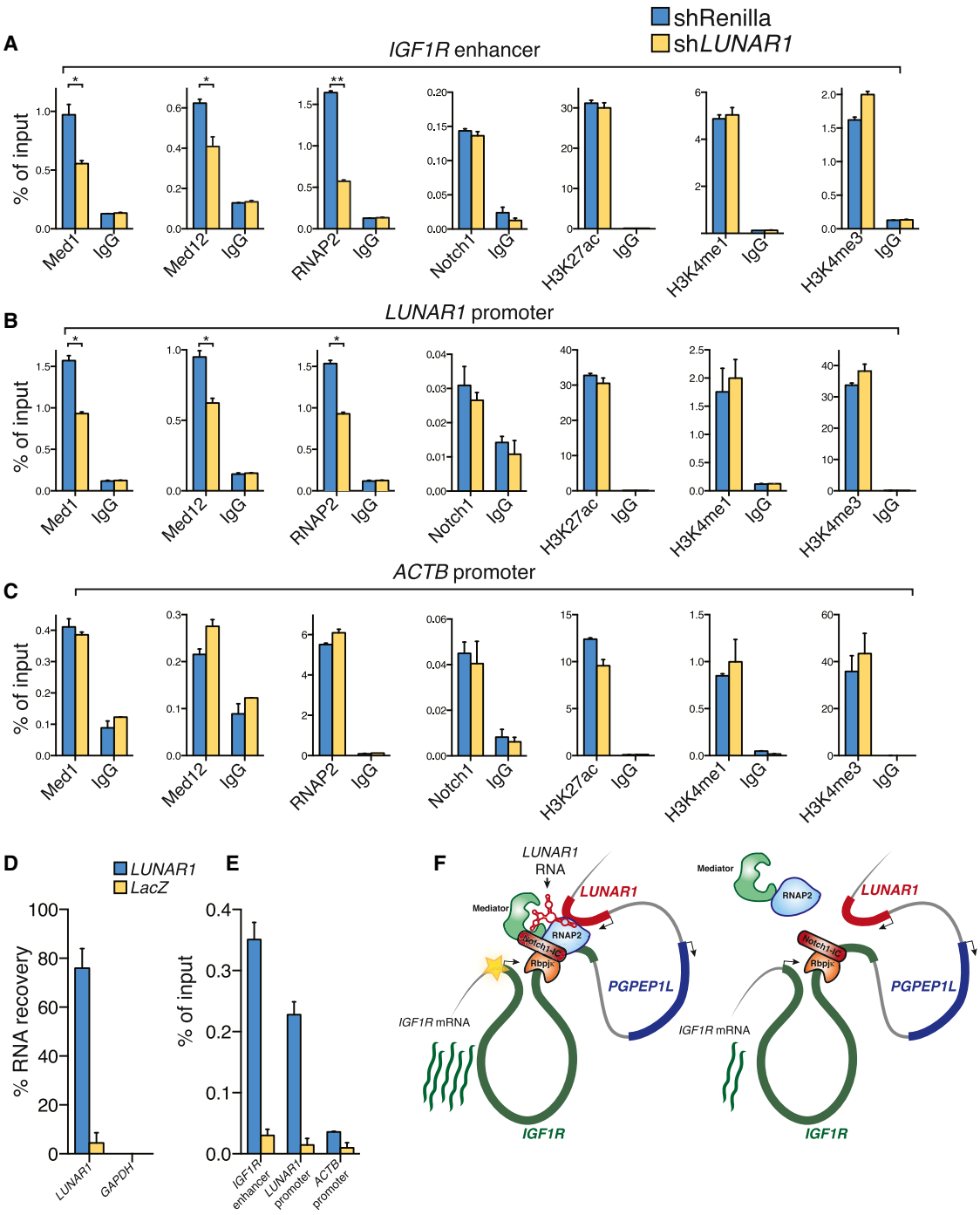

Figure 7. *LUNAR1* Modulates Mediator and RNA PolII Binding at the *IGF1R* Enhancer

(A–C) ChIP assays for MED1, MED12, RNAP2, NOTCH1, H3K27ac, H3K4me1, and H3K4me3 in T-ALL cells harboring nontargeting (blue) or *LUNAR1*-specific shRNAs followed by locus-specific qPCR at (A) *IGF1R* enhancer, (B) *LUNAR1* promoter, or (C) *ACTB* promoter.

(D) Percent recovery of *LUNAR1* following ChIRP.

(E) ChIRP assay using probes targeting *LUNAR1* (blue) or *LacZ* (yellow) followed by qPCR at the *IGF1R* enhancer, *LUNAR1* promoter, and *ACTB* promoter.

(F) A model for *cis*-regulation of gene expression by *LUNAR1*.

Error bars represent SEM of at least three experiments. * indicates p value < 0.05. ** indicates p value < 0.01.

Among enhancer-like lncRNAs, there appear to be two distinct functional mechanisms at play. One mechanism involves lncRNA-dependent recruitment of WDR5-containing methyltransferase complexes, which catalyzed methylation of the tails of histone 3 on lysine 4 (Gomez et al., 2013; Wang et al., 2011b; Yang et al., 2014). A second mechanism involves stabilization of Mediator complexes and RNA PolII at enhancer elements (Lai et al., 2013). Based on chromatin experiments following *LUNAR1* depletion, this lncRNA is most likely functionally similar to the noncoding RNA activators (nc-RNA-a) that have been described previously (Lai et al., 2013; Ørom et al., 2010). Because there are currently no methods for predicting lncRNA function based on sequence alone, we believe our results represent an incremental, yet important contribution to the overall understanding of lncRNA biology.

Our mapping of lncRNAs in human T-ALL opens the possibility that such previously uncharacterized transcripts are key modulators of cellular transformation, through their interaction with oncogenic and tumor suppressor programs in leukemia. Additionally, the suggested (and reported also here) tissue and cell-type specificity of lncRNA expression would suggest that such transcripts could be powerful and specific biomarkers used to categorize cancer subtypes and stratify patients for clinical trials and therapeutic protocols.

EXPERIMENTAL PROCEDURES

RNA Extraction Preparation for Next-Generation Sequencing

Total RNA was extracted from samples using the RNeasy Plus mini kit (Life Technologies, Carlsbad, CA, USA). Samples were then subject to poly(A) selection (Figures 1E, 5F, and 5G only) using oligo-dT beads (Life Technologies) or rRNA removal (all other samples) using the Ribo-Zero kit (Epicenter, Madison, WI, USA), according to the manufacturer's instructions. The resulting RNA samples were then used as input for library construction using the dUTP method as described (Parkhomchuk et al., 2009). RNA libraries were then sequenced on the Illumina HiSeq 2000 or 2500 using 50 bp paired-end reads.

RNA-Sequencing Data Analysis

All RNA-seq data were aligned to hg19 using TopHat (Trapnell et al., 2009) v1.4 with default parameters. We used Cuffdiff (Trapnell et al., 2010) v1.3 for all differential expression (DE) analyses with our custom annotation consisting of RefSeq entries plus T-ALL lncRNAs as described below. In all DE tests, a gene was considered significant if the q value was less than 0.05 (Cuffdiff default).

lncRNA Discovery

We sequenced two samples from T-ALL cell lines (CUTLL1 and HPBALL), two primary human thymus samples to ultra-high depth (>200 million mate pairs each), ten primary pediatric T-ALL samples (60–80 million mate pairs each), and data generated by the Roadmap Epigenomics project for Naive $CD4^+$ and $CD8^+$ T cells to be used for ab initio transcriptome assembly with Cufflinks v1.3. Briefly, Cufflinks was run with the following options: -u, -N, -g (RefSeq GTF file provided as guide), and -M (rRNA and 7SK RNA mask file provided). We generated transcriptome assemblies for each of these samples separately and then used Cuffmerge to combine all annotations. For all subsequent filtering and processing steps, please see the Extended Experimental Procedures.

ChIP

The following antibodies were used for ChIP experiments: Notch1 C-20 (Santa Cruz sc-6014), Med1 (Bethyl, A300-793A), Med12 (Bethyl, A300-774A), RNA PolII N-20 (Santa Cruz, sc-899), H3K4me1 (Abcam, ab8895), H3K4me3 (Active Motif, 39159), and H3K27ac (Abcam, ab4729). ChIP assays were performed essentially as described previously (Whyte et al., 2013). See the Extended Experimental Procedures for a detailed description of ChIP assay.

ChIRP

ChIRP assays were performed as described (Chu et al., 2011) with the following modifications. Cells were double crosslinked first with 2 mM EGS for 45 min at room temperature and washed twice with ice-cold PBS. Cells were then further cross-liked with 3% formaldehyde for 30 min at room temperature, and reaction was stopped by the addition of 0.125M glycine followed by two more washes in PBS. Crosslinked cells were then lysed in sonication buffer (see ChIP method) supplemented with SUPERaseIn (Life technologies), and chromatin was sheared exactly as for ChIP assays. Chromatin was cleared by centrifugation and supernatant was used for ChIRP reactions. All following steps were performed exactly as described by Chu et al. with the following exceptions: in the hybridization buffer, 1% Triton with 0.1% SDS was used instead of 1% SDS, and in the wash buffer, SDS concentration was lowered from 0.5% to 0.1%. Probes used for ChIRP assays are listed in Table S2.

Chromosome Conformation Capture

3C experiments were performed essentially as described previously (Hagège et al., 2007). Please see the Extended Experimental Procedures for a detailed description of this method.

ACCESSION NUMBERS

The NCBI Gene Expression Omnibus accession number for the RNA-Seq data reported in this paper is GSE57982.

SUPPLEMENTAL INFORMATION

Supplemental Information includes Extended Experimental Procedures, five figures, and four tables and can be found with this article online at http://dx.doi.org/10.1016/j.cell.2014.05.049.

ACKNOWLEDGMENTS

We would like to thank the members of the I.A. laboratory for helpful discussions throughout the duration of the project. We thank Drs. Danny Reinberg, Roberto Bonasio, Howard Chang, and Adam Schmidtt for valuable discussions, technical advice, and reagents. We thank Drs. Sergei Koralov and Jane Skok for their continued support and helpful insight. We are grateful to Dr. Mignon Loh and the Children's Oncology Group for providing patient samples and to Dr. A. Heguy and the NYU Genome Technology Center (supported in part by NIH/NCI P30 CA016087-30 grant) for assistance with sequencing experiments. Research is supported by the Chair's Grant U10 CA98543 and Human Specimen Banking Grant U24 CA114766 of the Children's Oncology Group from the National Cancer Institute, National Institutes of Health (Bethesda, MD, USA). I.A. was supported by the National Institutes of Health (1RO1CA133379, 1RO1CA105129, 1RO1CA149655, 5RO1CA173636, 5RO1CA169784, and 1RO1GM088847). I.A. was also supported by the William Lawrence and Blanche Hughes Foundation, The Leukemia & Lymphoma Society (TRP#6340-11, LLS#6373-13), The Chemotherapy Foundation, The Irma T. Hirschl Trust, The V Foundation for Cancer Research, and the St. Baldrick's Foundation. T.T. is supported by NIH training grants 5T32CA009161-37 and 5T32GM0072-38. I.A. is a Howard Hughes Medical Institute Early Career Scientist. A.T. carried out a portion of this work while at the Computational Biology Center, IBM Research (Yorktown Heights, NY, USA). P.N. is supported by an American Society of Hematology fellowship.

Received: August 26, 2013
Revised: March 23, 2014
Accepted: May 16, 2014
Published: July 31, 2014

REFERENCES

Almada, A.E., Wu, X., Kriz, A.J., Burge, C.B., and Sharp, P.A. (2013). Promoter directionality is controlled by U1 snRNP and polyadenylation signals. Nature *499*, 360–363.

Boumil, R.M., and Lee, J.T. (2001). Forty years of decoding the silence in X-chromosome inactivation. Hum. Mol. Genet. *10*, 2225–2232.

Cabili, M.N., Trapnell, C., Goff, L., Koziol, M., Tazon-Vega, B., Regev, A., and Rinn, J.L. (2011). Integrative annotation of human large intergenic noncoding RNAs reveals global properties and specific subclasses. Genes Dev. *25*, 1915–1927.

Carninci, P., Kasukawa, T., Katayama, S., Gough, J., Frith, M.C., Maeda, N., Oyama, R., Ravasi, T., Lenhard, B., Wells, C., et al.; FANTOM Consortium; RIKEN Genome Exploration Research Group and Genome Science Group (Genome Network Project Core Group) (2005). The transcriptional landscape of the mammalian genome. Science *309*, 1559–1563.

Chu, C., Qu, K., Zhong, F.L., Artandi, S.E., and Chang, H.Y. (2011). Genomic maps of long noncoding RNA occupancy reveal principles of RNA-chromatin interactions. Mol. Cell *44*, 667–678.

Clark, M.B., Amaral, P.P., Schlesinger, F.J., Dinger, M.E., Taft, R.J., Rinn, J.L., Ponting, C.P., Stadler, P.F., Morris, K.V., Morillon, A., et al. (2011). The reality of pervasive transcription. PLoS Biol. *9*, e1000625, discussion e1001102.

De Keersmaecker, K., Atak, Z.K., Li, N., Vicente, C., Patchett, S., Girardi, T., Gianfelici, V., Geerdens, E., Clappier, E., Porcu, M., et al. (2013). Exome sequencing identifies mutation in CNOT3 and ribosomal genes RPL5 and RPL10 in T-cell acute lymphoblastic leukemia. Nat. Genet. *45*, 186–190.

Dixon, J.R., Selvaraj, S., Yue, F., Kim, A., Li, Y., Shen, Y., Hu, M., Liu, J.S., and Ren, B. (2012). Topological domains in mammalian genomes identified by analysis of chromatin interactions. Nature *485*, 376–380.

Djebali, S., Davis, C.A., Merkel, A., Dobin, A., Lassmann, T., Mortazavi, A., Tanzer, A., Lagarde, J., Lin, W., Schlesinger, F., et al. (2012). Landscape of transcription in human cells. Nature *489*, 101–108.

Du, Z., Fei, T., Verhaak, R.G., Su, Z., Zhang, Y., Brown, M., Chen, Y., and Liu, X.S. (2013). Integrative genomic analyses reveal clinically relevant long noncoding RNAs in human cancer. Nat. Struct. Mol. Biol. *20*, 908–913.

Engreitz, J.M., Pandya-Jones, A., McDonel, P., Shishkin, A., Sirokman, K., Surka, C., Kadri, S., Xing, J., Goren, A., Lander, E.S., et al. (2013). The Xist lncRNA exploits three-dimensional genome architecture to spread across the X chromosome. Science *341*, 1237973.

Fabbri, G., Rasi, S., Rossi, D., Trifonov, V., Khiabanian, H., Ma, J., Grunn, A., Fangazio, M., Capello, D., Monti, S., et al. (2011). Analysis of the chronic lymphocytic leukemia coding genome: role of NOTCH1 mutational activation. J. Exp. Med. *208*, 1389–1401.

Ferrando, A.A. (2009). The role of NOTCH1 signaling in T-ALL. Hematology (Am. Soc. Hematol. Educ. Program), 353–361.

Ferrando, A.A., Neuberg, D.S., Staunton, J., Loh, M.L., Huard, C., Raimondi, S.C., Behm, F.G., Pui, C.H., Downing, J.R., Gilliland, D.G., et al. (2002). Gene expression signatures define novel oncogenic pathways in T cell acute lymphoblastic leukemia. Cancer Cell *1*, 75–87.

Fragoso, R., Mao, T., Wang, S., Schaffert, S., Gong, X., Yue, S., Luong, R., Min, H., Yashiro-Ohtani, Y., Davis, M., et al. (2012). Modulating the strength and threshold of NOTCH oncogenic signals by mir-181a-1/b-1. PLoS Genet. *8*, e1002855.

Garding, A., Bhattacharya, N., Claus, R., Ruppel, M., Tschuch, C., Filarsky, K., Idler, I., Zucknick, M., Caudron-Herger, M., Oakes, C., et al. (2013). Epigenetic upregulation of lncRNAs at 13q14.3 in leukemia is linked to the In Cis downregulation of a gene cluster that targets NF-kB. PLoS Genet. *9*, e1003373.

Gomez, J.A., Wapinski, O.L., Yang, Y.W., Bureau, J.F., Gopinath, S., Monack, D.M., Chang, H.Y., Brahic, M., and Kirkegaard, K. (2013). The NeST long ncRNA controls microbial susceptibility and epigenetic activation of the interferon-γ locus. Cell *152*, 743–754.

Grote, P., Wittler, L., Hendrix, D., Koch, F., Währisch, S., Beisaw, A., Macura, K., Bläss, G., Kellis, M., Werber, M., and Herrmann, B.G. (2013). The tissue-specific lncRNA Fendrr is an essential regulator of heart and body wall development in the mouse. Dev. Cell *24*, 206–214.

Gupta, R.A., Shah, N., Wang, K.C., Kim, J., Horlings, H.M., Wong, D.J., Tsai, M.C., Hung, T., Argani, P., Rinn, J.L., et al. (2010). Long non-coding RNA HOTAIR reprograms chromatin state to promote cancer metastasis. Nature *464*, 1071–1076.

Guttman, M., Amit, I., Garber, M., French, C., Lin, M.F., Feldser, D., Huarte, M., Zuk, O., Carey, B.W., Cassady, J.P., et al. (2009). Chromatin signature reveals over a thousand highly conserved large non-coding RNAs in mammals. Nature *458*, 223–227.

Guttman, M., Donaghey, J., Carey, B.W., Garber, M., Grenier, J.K., Munson, G., Young, G., Lucas, A.B., Ach, R., Bruhn, L., et al. (2011). lincRNAs act in the circuitry controlling pluripotency and differentiation. Nature *477*, 295–300.

Guttman, M., Russell, P., Ingolia, N.T., Weissman, J.S., and Lander, E.S. (2013). Ribosome profiling provides evidence that large noncoding RNAs do not encode proteins. Cell *154*, 240–251.

Hagège, H., Klous, P., Braem, C., Splinter, E., Dekker, J., Cathala, G., de Laat, W., and Forné, T. (2007). Quantitative analysis of chromosome conformation capture assays (3C-qPCR). Nat. Protoc. *2*, 1722–1733.

Harrow, J., Frankish, A., Gonzalez, J.M., Tapanari, E., Diekhans, M., Kokocinski, F., Aken, B.L., Barrell, D., Zadissa, A., Searle, S., et al. (2012). GENCODE: the reference human genome annotation for The ENCODE Project. Genome Res. *22*, 1760–1774.

Heintzman, N.D., Hon, G.C., Hawkins, R.D., Kheradpour, P., Stark, A., Harp, L.F., Ye, Z., Lee, L.K., Stuart, R.K., Ching, C.W., et al. (2009). Histone modifications at human enhancers reflect global cell-type-specific gene expression. Nature *459*, 108–112.

Huarte, M., Guttman, M., Feldser, D., Garber, M., Koziol, M.J., Kenzelmann-Broz, D., Khalil, A.M., Zuk, O., Amit, I., Rabani, M., et al. (2010). A large intergenic noncoding RNA induced by p53 mediates global gene repression in the p53 response. Cell *142*, 409–419.

Hung, T., Wang, Y., Lin, M.F., Koegel, A.K., Kotake, Y., Grant, G.D., Horlings, H.M., Shah, N., Umbricht, C., Wang, P., et al. (2011). Extensive and coordinated transcription of noncoding RNAs within cell-cycle promoters. Nat. Genet. *43*, 621–629.

Imakaev, M., Fudenberg, G., McCord, R.P., Naumova, N., Goloborodko, A., Lajoie, B.R., Dekker, J., and Mirny, L.A. (2012). Iterative correction of Hi-C data reveals hallmarks of chromosome organization. Nat. Methods *9*, 999–1003.

Katayama, S., Tomaru, Y., Kasukawa, T., Waki, K., Nakanishi, M., Nakamura, M., Nishida, H., Yap, C.C., Suzuki, M., Kawai, J., et al.; RIKEN Genome Exploration Research Group; Genome Science Group (Genome Network Project Core Group); FANTOM Consortium (2005). Antisense transcription in the mammalian transcriptome. Science *309*, 1564–1566.

King, B., Trimarchi, T., Reavie, L., Xu, L., Mullenders, J., Ntziachristos, P., Aranda-Orgilles, B., Perez-Garcia, A., Shi, J., Vakoc, C., et al. (2013). The ubiquitin ligase FBXW7 modulates leukemia-initiating cell activity by regulating MYC stability. Cell *153*, 1552–1566.

Klattenhoff, C.A., Scheuermann, J.C., Surface, L.E., Bradley, R.K., Fields, P.A., Steinhauser, M.L., Ding, H., Butty, V.L., Torrey, L., Haas, S., et al. (2013). Braveheart, a long noncoding RNA required for cardiovascular lineage commitment. Cell *152*, 570–583.

Kopan, R., and Ilagan, M.X. (2009). The canonical Notch signaling pathway: unfolding the activation mechanism. Cell *137*, 216–233.

Kretz, M., Siprashvili, Z., Chu, C., Webster, D.E., Zehnder, A., Qu, K., Lee, C.S., Flockhart, R.J., Groff, A.F., Chow, J., et al. (2013). Control of somatic tissue differentiation by the long non-coding RNA TINCR. Nature *493*, 231–235.

Lai, F., Orom, U.A., Cesaroni, M., Beringer, M., Taatjes, D.J., Blobel, G.A., and Shiekhattar, R. (2013). Activating RNAs associate with Mediator to enhance chromatin architecture and transcription. Nature *494*, 497–501.

Lee, C.S., Ungewickell, A., Bhaduri, A., Qu, K., Webster, D.E., Armstrong, R., Weng, W.K., Aros, C.J., Mah, A., Chen, R.O., et al. (2012). Transcriptome

sequencing in Sezary syndrome identifies Sezary cell and mycosis fungoides-associated lncRNAs and novel transcripts. Blood *120*, 3288–3297.

Lee, J.T. (2012). Epigenetic regulation by long noncoding RNAs. Science *338*, 1435–1439.

Li, W., Notani, D., Ma, Q., Tanasa, B., Nunez, E., Chen, A.Y., Merkurjev, D., Zhang, J., Ohgi, K., Song, X., et al. (2013). Functional roles of enhancer RNAs for oestrogen-dependent transcriptional activation. Nature *498*, 516–520.

Li, X., Sanda, T., Look, A.T., Novina, C.D., and von Boehmer, H. (2011). Repression of tumor suppressor miR-451 is essential for NOTCH1-induced oncogenesis in T-ALL. J. Exp. Med. *208*, 663–675.

Lieberman-Aiden, E., van Berkum, N.L., Williams, L., Imakaev, M., Ragoczy, T., Telling, A., Amit, I., Lajoie, B.R., Sabo, P.J., Dorschner, M.O., et al. (2009). Comprehensive mapping of long-range interactions reveals folding principles of the human genome. Science *326*, 289–293.

Lin, M.F., Jungreis, I., and Kellis, M. (2011). PhyloCSF: a comparative genomics method to distinguish protein coding and non-coding regions. Bioinformatics *27*, i275–i282.

Loewer, S., Cabili, M.N., Guttman, M., Loh, Y.H., Thomas, K., Park, I.H., Garber, M., Curran, M., Onder, T., Agarwal, S., et al. (2010). Large intergenic non-coding RNA-RoR modulates reprogramming of human induced pluripotent stem cells. Nat. Genet. *42*, 1113–1117.

Look, A.T. (2004). Molecular pathways in T-cell acute lympho-blastic leukemia: ramifications for therapy. Clin. Adv. Hematol. Oncol. *2*, 779–780.

Medyouf, H., Gusscott, S., Wang, H., Tseng, J.C., Wai, C., Nemirovsky, O., Trumpp, A., Pflumio, F., Carboni, J., Gottardis, M., et al. (2011). High-level IGF1R expression is required for leukemia-initiating cell activity in T-ALL and is supported by Notch signaling. J. Exp. Med. *208*, 1809–1822.

Ntziachristos, P., Tsirigos, A., Van Vlierberghe, P., Nedjic, J., Trimarchi, T., Flaherty, M.S., Ferres-Marco, D., da Ros, V., Tang, Z., Siegle, J., et al. (2012). Genetic inactivation of the polycomb repressive complex 2 in T cell acute lymphoblastic leukemia. Nat. Med. *18*, 298–301.

Ørom, U.A., Derrien, T., Beringer, M., Gumireddy, K., Gardini, A., Bussotti, G., Lai, F., Zytnicki, M., Notredame, C., Huang, Q., et al. (2010). Long noncoding RNAs with enhancer-like function in human cells. Cell *143*, 46–58.

Palomero, T., Barnes, K.C., Real, P.J., Glade Bender, J.L., Sulis, M.L., Murty, V.V., Colovai, A.I., Balbin, M., and Ferrando, A.A. (2006). CUTLL1, a novel human T-cell lymphoma cell line with t(7;9) rearrangement, aberrant NOTCH1 activation and high sensitivity to gamma-secretase inhibitors. Leukemia *20*, 1279–1287.

Parkhomchuk, D., Borodina, T., Amstislavskiy, V., Banaru, M., Hallen, L., Krobitsch, S., Lehrach, H., and Soldatov, A. (2009). Transcriptome analysis by strand-specific sequencing of complementary DNA. Nucleic Acids Res. *37*, e123.

Prensner, J.R., Iyer, M.K., Balbin, O.A., Dhanasekaran, S.M., Cao, Q., Brenner, J.C., Laxman, B., Asangani, I.A., Grasso, C.S., Kominsky, H.D., et al. (2011). Transcriptome sequencing across a prostate cancer cohort identifies PCAT-1, an unannotated lincRNA implicated in disease progression. Nat. Biotechnol. *29*, 742–749.

Prensner, J.R., Iyer, M.K., Sahu, A., Asangani, I.A., Cao, Q., Patel, L., Vergara, I.A., Davicioni, E., Erho, N., Ghadessi, M., et al. (2013). The long noncoding RNA SChLAP1 promotes aggressive prostate cancer and antagonizes the SWI/SNF complex. Nat. Genet. *45*, 1392–1398.

Rada-Iglesias, A., Bajpai, R., Swigut, T., Brugmann, S.A., Flynn, R.A., and Wysocka, J. (2011). A unique chromatin signature uncovers early developmental enhancers in humans. Nature *470*, 279–283.

Rinn, J.L., and Chang, H.Y. (2012). Genome regulation by long noncoding RNAs. Annu. Rev. Biochem. *81*, 145–166.

Rinn, J.L., Kertesz, M., Wang, J.K., Squazzo, S.L., Xu, X., Brugmann, S.A., Goodnough, L.H., Helms, J.A., Farnham, P.J., Segal, E., and Chang, H.Y. (2007). Functional demarcation of active and silent chromatin domains in human HOX loci by noncoding RNAs. Cell *129*, 1311–1323.

Seila, A.C., Calabrese, J.M., Levine, S.S., Yeo, G.W., Rahl, P.B., Flynn, R.A., Young, R.A., and Sharp, P.A. (2008). Divergent transcription from active promoters. Science *322*, 1849–1851.

Sigova, A.A., Mullen, A.C., Molinie, B., Gupta, S., Orlando, D.A., Guenther, M.G., Almada, A.E., Lin, C., Sharp, P.A., Giallourakis, C.C., and Young, R.A. (2013). Divergent transcription of long noncoding RNA/mRNA gene pairs in embryonic stem cells. Proc. Natl. Acad. Sci. USA *110*, 2876–2881.

Trapnell, C., Pachter, L., and Salzberg, S.L. (2009). TopHat: discovering splice junctions with RNA-Seq. Bioinformatics *25*, 1105–1111.

Trapnell, C., Williams, B.A., Pertea, G., Mortazavi, A., Kwan, G., van Baren, M.J., Salzberg, S.L., Wold, B.J., and Pachter, L. (2010). Transcript assembly and quantification by RNA-Seq reveals unannotated transcripts and isoform switching during cell differentiation. Nat. Biotechnol. *28*, 511–515.

Tsai, M.C., Manor, O., Wan, Y., Mosammaparast, N., Wang, J.K., Lan, F., Shi, Y., Segal, E., and Chang, H.Y. (2010). Long noncoding RNA as modular scaffold of histone modification complexes. Science *329*, 689–693.

Ulitsky, I., and Bartel, D.P. (2013). lincRNAs: genomics, evolution, and mechanisms. Cell *154*, 26–46.

Vaquero, A., Scher, M., Lee, D., Erdjument-Bromage, H., Tempst, P., and Reinberg, D. (2004). Human SirT1 interacts with histone H1 and promotes formation of facultative heterochromatin. Mol. Cell *16*, 93–105.

Wang, H., Zou, J., Zhao, B., Johannsen, E., Ashworth, T., Wong, H., Pear, W.S., Schug, J., Blacklow, S.C., Arnett, K.L., et al. (2011a). Genome-wide analysis reveals conserved and divergent features of Notch1/RBPJ binding in human and murine T-lymphoblastic leukemia cells. Proc. Natl. Acad. Sci. USA *108*, 14908–14913.

Wang, K.C., Yang, Y.W., Liu, B., Sanyal, A., Corces-Zimmerman, R., Chen, Y., Lajoie, B.R., Protacio, A., Flynn, R.A., Gupta, R.A., et al. (2011b). A long noncoding RNA maintains active chromatin to coordinate homeotic gene expression. Nature *472*, 120–124.

Weng, A.P., Ferrando, A.A., Lee, W., Morris, J.P., 4th, Silverman, L.B., Sanchez-Irizarry, C., Blacklow, S.C., Look, A.T., and Aster, J.C. (2004). Activating mutations of NOTCH1 in human T cell acute lymphoblastic leukemia. Science *306*, 269–271.

Whyte, W.A., Orlando, D.A., Hnisz, D., Abraham, B.J., Lin, C.Y., Kagey, M.H., Rahl, P.B., Lee, T.I., and Young, R.A. (2013). Master transcription factors and mediator establish super-enhancers at key cell identity genes. Cell *153*, 307–319.

Yang, L., Lin, C., Liu, W., Zhang, J., Ohgi, K.A., Grinstein, J.D., Dorrestein, P.C., and Rosenfeld, M.G. (2011). ncRNA- and Pc2 methylation-dependent gene relocation between nuclear structures mediates gene activation programs. Cell *147*, 773–788.

Yang, L., Lin, C., Jin, C., Yang, J.C., Tanasa, B., Li, W., Merkurjev, D., Ohgi, K.A., Meng, D., Zhang, J., et al. (2013). lncRNA-dependent mechanisms of androgen-receptor-regulated gene activation programs. Nature *500*, 598–602.

Yang, Y.W., Flynn, R.A., Chen, Y., Qu, K., Wan, B., Wang, K.C., Lei, M., and Chang, H.Y. (2014). Essential role of lncRNA binding for WDR5 maintenance of active chromatin and embryonic stem cell pluripotency. Elife *3*, e02046.

Yildirim, E., Kirby, J.E., Brown, D.E., Mercier, F.E., Sadreyev, R.I., Scadden, D.T., and Lee, J.T. (2013). Xist RNA is a potent suppressor of hematologic cancer in mice. Cell *152*, 727–742.

Yu, L., Slovak, M.L., Mannoor, K., Chen, C., Hunger, S.P., Carroll, A.J., Schultz, R.A., Shaffer, L.G., Ballif, B.C., and Ning, Y. (2011). Microarray detection of multiple recurring submicroscopic chromosomal aberrations in pediatric T-cell acute lymphoblastic leukemia. Leukemia *25*, 1042–1046.

Zhang, J., Ding, L., Holmfeldt, L., Wu, G., Heatley, S.L., Payne-Turner, D., Easton, J., Chen, X., Wang, J., Rusch, M., et al. (2012). The genetic basis of early T-cell precursor acute lymphoblastic leukaemia. Nature *481*, 157–163.